Nuclear Physics A569 (1994) 333c–342c
North-Holland, Amsterdam

NUCLEAR PHYSICS A

Microscopic origin of the giant resonance structure

V.Yu. Ponomarev[a,b], E. Vigezzi[a], P.F. Bortignon[a,c], R.A. Broglia[a,c,d], G. Colò[a,c], G. Lazzari[a,c], V.V. Voronov[b] and G. Baur[e]

[a]Istituto Nazionale di Fisica Nucleare, Sezione di Milano, Via Celoria 16, 20133 Milano, Italy

[b]Laboratory of Theoretical Physics, Joint Institute for Nuclear Research, Dubna, Head Post Office, P. O. Box 79, Moscow, Russia

[c]Dipartimento di Fisica, Università di Milano, Via Celoria 16, 20133 Milano, Italy

[d]The Niels Bohr Institute, University of Copenhagen, Blegdamsvej 17, 2100 Copenhagen Ø, Denmark

[e]Institut für Kernphysik, Forschungzentrum Jülich GmbH, Germany

Microscopic calculations of the fine structure of giant resonances for spherical nuclei are presented. Excited states are described by wave functions which take into account the coupling of simple one-phonon configurations with two-phonon states. Few examples are presented: the γ-decay of resonances to the ground and low-lying excited states and the relativistic Coulomb excitation of the double giant dipole resonance states.

1. INTRODUCTION

In the last few years, the experimental study of giant resonances, [1], has benefitted from the use of large, "full" geometry detectors and of more and more heavy and energetic beams. The particle and γ-decay have been studied, branching ratios obtained, the direct and the statistical component of the decay processes resolved [2]. These exclusive data require rather complete theoretical models to be explained [3-4]. One of them will be presented and used in this work.

2. FORMALISM AND DETAILS OF CALCULATIONS

The calculations presented below have been carried out within the Quasiparticle Phonon Model (QPM) [5-7]. The model Hamiltonian $\mathcal{H}$ includes an average field $V_{p(n)}$

0375-9474/94/$07.00
SSDI 0375-9474(94)00035-L

for protons and neutrons, a monopole pairing interaction and isoscalar and isovector residual interaction of a separable type with a form factor proportional to $dV_{p(n)}/dr$. Excited states of even-even nuclei are treated in terms of phonon excitations built upon the ground state which is considered as a phonon vacuum $|0>_{ph}$. The phonon creation operators $Q^+_{\lambda\mu i}$ of multipolarity $\lambda\mu$ are defined as a linear combination of two quasiparticle creation α^+_{jm} and annihilation α_{jm} operators labelled by the single-particle quantum numbers jm of the average field V as follows:

$$Q^+_{\lambda\mu i} = \frac{1}{2}\sum_{j\,j'}^{p,n}\left\{\psi^{\lambda i}_{jj'}[\alpha^+_{jm}\alpha^+_{j'm'}]_{\lambda\mu} + (-1)^{\lambda-\mu}\phi^{\lambda i}_{jj'}[\alpha_{jm}\alpha_{j'm'}]_{\lambda-\mu}\right\}\ , \tag{1}$$

where

$$[\alpha^+_{jm}\alpha^+_{j'm'}]_{\lambda\mu} = \sum_{mm'} < jmj'm'|\lambda\mu > \alpha^+_{jm}\alpha^+_{j'm'}\ .$$

The forwardgoing $\psi^{\lambda i}_{jj'}$ and backwardgoing $\phi^{\lambda i}_{jj'}$ amplitudes are obtained by solving the random phase approximation (RPA) equations that yield a set of one-phonon configurations with excitation energies $\omega_{\lambda i}$ for the i-th root. Among phonons we obtain both collective and non-collective states which essentially correspond to pure two-quasiparticle excitations.

The mixing of one-phonon configurations, through which giant resonances are excited in inelastic scattering, with more complex configurations is strong in the resonance region, because of the high density of states. Thus, we write the wave function of resonance states as a sum of configurations of increasing number of phonons. If we limit this sum to one- and two-phonon configurations, the wave function for the λ^π_ν–state has the form:

$$\Psi_\nu(\lambda\mu) = \{\sum_i R_i(\lambda\nu)Q^+_{\lambda\mu i} + \sum_{\lambda_1 i_1 \lambda_2 i_2} P^{\lambda_2 i_2}_{\lambda_1 i_1}(\lambda\nu)\left[Q^+_{\lambda_1\mu_1 i_1}Q^+_{\lambda_2\mu_2 i_2}\right]_{\lambda\mu}\}|0>_{ph}\ . \tag{2}$$

In actual calculations we do not include configurations with two non-collective phonons. By this truncation of the two-phonon basis, we remove complex configurations that are weakly coupled to one-phonon states and, on the other hand, may strongly violate the Pauli principle.

To obtain the amplitudes $R_i(\lambda\nu)$ and $P^{\lambda_2 i_2}_{\lambda_1 i_1}(\lambda\nu)$, we diagonalize the model Hamiltonian on the basis of wave functions (2). Eigenvalues E_ν are obtained as the roots of the following determinantal equation:

$$F(E_\nu) = det|(\omega_{\lambda i} - E_\nu)\delta_{ii'} - \frac{1}{2}\sum_{\lambda_1 i_1, \lambda_2 i_2}\frac{U^{\lambda_2 i_2}_{\lambda_1 i_1}(\lambda i)U^{\lambda_2 i_2}_{\lambda_1 i_1}(\lambda i')}{\omega_{\lambda_1 i_1} + \omega_{\lambda_2 i_2} - E_\nu}| = 0\ , \tag{3}$$

where

$$U^{\lambda_2 i_2}_{\lambda_1 i_1}(\lambda i) =< Q_{\lambda i}||\mathcal{H}||\left[Q^+_{\lambda_1 i_1}Q^+_{\lambda_2 i_2}\right]_\lambda >$$

is the matrix element of the interaction between one- and two-phonon configurations. The rank of the determinant (3) is determined by the number of one-phonon configurations included in the first term of the wave function (2).

Numerical calculations have been performed with the Woods-Saxon potential as the average field with the parameters from ref. [7]. Parameters of the residual interactions were adjusted to the properties of the low-lying collective levels. Natural parity phonons with $\lambda^\pi = 1^-$ - 8^+ have been included in the two-phonon term of the wave function (2).

3. SINGLE RESONANCES

Giant resonances are not broad featureless structures, but it is possible to study experimentally physical processes in which different states from the resonance region are excited by different probes, and by measuring the decay properties of these states with coincidence techniques, fingerprints of some specific states may be observed. Such experiments can be understood within the detailed microscopic description introduced above, which considers giant resonances as a set of a large number of states, with their own properties.

3.1. Fine structure of the GDR

As a first example, let us discuss the fragmentation of the B(Eλ) strength due to the coupling of one-phonon configurations to two-phonon ones in the resonance region. We take as an example the giant dipole resonance (GDR) in ^{136}Xe. Figure 1 presents the B(E1) strength distribution over one-phonon configurations. The major fraction of the B(E1) strength is carried by these configurations, the direct excitation of two-phonon 1^- states from the ground state being about three orders of magnitude weaker. The one-phonon states exhaust 107% of the classical oscillator strength.

Of these, 20 states have an oscillator strength which is at least 1% of the strongest strength and together exhaust 104% of the classical EWSR. We have used these states in the coupling to two-phonon components with energy lower or equal to 21 MeV, obtaining 2632 two–phonon configurations. One obtains 1614 states of type (2), in the energy interval from 7 MeV to 19.5 MeV. The B(E1) value associated with each mixed state is calculated through its admixture with one-phonon states, as $| < \nu||M(E1)||0 > |^2 = |\sum_i R_i(\nu) < 0||Q_{1^-i}M(E1)||0 > |^2$. The coupling of simple (one-phonon) configurations to more complex (two-phonon) ones results in a strong fragmentation. The values of the centroid and width of the strength distribution are $E_{GDR} = 15.1$ MeV and $\Gamma_{GDR} = 4$ MeV.

This example clearly shows how the width of a giant resonance arises theoretically. Calculations with the set of wave functions of eq. (2), underestimate by a few hundred of keV the experimentally measured widths of giant resonances. This is not surprising since configurations more complex than two-phonon ones are not included.

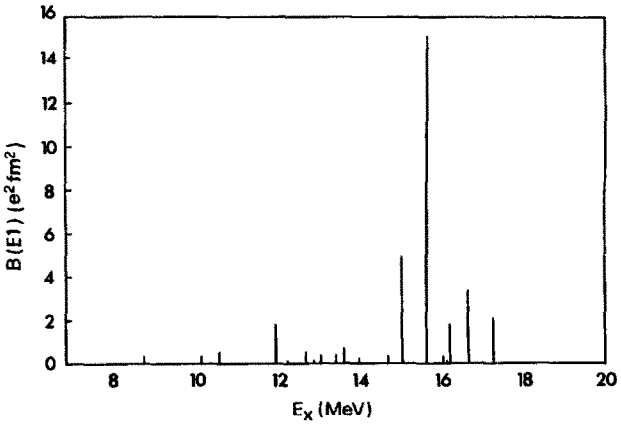

Fig. 1. GDR in ^{136}Xe. E1-strength distribution over one-phonon configurations resulting from the RPA solution.

3.2. Substructures of the (γ,n)Pb cross section

Some substructures of the GDR have been observed in the (γ,n) cross sections at low excitation energies [8]. The experimental $(\gamma,n)^{208}$Pb cross section is presented in the left part of Figure 2. It is compared to the calculated cross section for the dipole photoabsorption

$$\sigma_{\gamma t}(E_\gamma) = 4.025\, E_\gamma\, b(E1, E_\gamma)\ , \tag{4}$$

where

$$b(E1,E) = \sum_\nu |< \nu||M(E1)||0 >|^2\, \frac{1}{2\pi}\ \frac{\Delta}{(E-E_\nu)^2 + \Delta^2/4} \tag{5}$$

is the dipole strength function (in units e^2fm^2) calculated introducing an averaging parameter Δ, the γ ray energy is in MeV and the cross section in millibarns. One can notice from Figure 2 a rather good agreement of experimental data with the theoretical calculations. The truncation of the large number of two phonon configurations which are weakly coupled with one-phonon states causes some overestimation of the cross section near its maximum and some underestimation of the high energy part.

The results of the RPA calculation for the dipole strength distribution are shown in the left figure by vertical lines. The coupling of the RPA collective states with the two-phonon states results in a redistribution of the dipole strength. This leads to pronounced substructures in the cross sections in the low energy part. The increase of the excitation

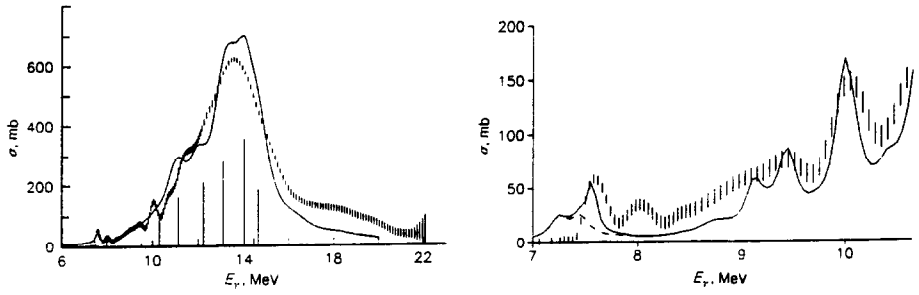

Fig. 2. Experimental and theoretical $(\gamma, n)^{208}$Pb cross section. Calculations are performed with $\Delta = 1$ MeV (left) and 0.2 MeV (right).

energy leads to the increase of the level density, and as a result, substructures disappear. One cannot observe any substructures in nuclei with open shells because of the high level densities and strong coupling between configurations [9].

To shed more light on the problem of the existence of substructures, the low energy part of the cross section has been calculated in the right part of Figure 2 with a smaller value for $\Delta = 0.2$ MeV. The main structures observed in the experiment at the excitation energies 7.6, 8.6, 9.1, 9.5, 10.0 and 11.3 MeV are reproduced. The solid curve includes the contribution of E1 and M1 photoabsorption, while the dashed curve shows the E1-contribution. It is noted that M1 transitions contribute essentially to the substructure at the energy 7.6 MeV. This result is in good agreement with the experimental M1 strength distribution measured with highly polarized tagged photons [10]. It is worth mentioning that E2 transitions do not give any noticeable contribution to the cross section.

3.3. γ-decay of the GDR into the ground and 2_1^+ states

Recently, ^{116,124}Sn$(\alpha, \alpha'\gamma)$ experiments have been performed at the KVI [11]. The GDR region of excitation was investigated. Coincidence measurements between the scattered α-particles and the emitted γ-rays were used to select the contribution of the GDR from the giant monopole (GMR) and quadrupole (GQR) resonances. It has been observed that the population of the first 2^+ excited state was nearly as strong as that of the ground state.

The following interpretation of these data has been proposed [12]. As soon as the GDR is excited by α particles it decays into the ground state by E1 transitions and to

the 2_1^+ state because of the strong coupling of the GDR with two-phonon configurations $[GDR \otimes 2_1^+]_{1^-}$.

In the calculation of the $(\alpha, \alpha'\gamma)$ cross sections the ideas of the multistep theory of nuclear reactions (see, e.g. [13]) have been applied and the $\sigma_{\alpha,\alpha'\gamma}(E)$ coincidence cross section has been deduced following the procedure described in ref. [14] as:

$$\sigma_{\alpha,\alpha'\gamma}(E) = \sigma_{\alpha,\alpha'}(E)\left[\frac{\Gamma_\gamma(E)}{\Gamma} + \frac{\Gamma^\downarrow}{\Gamma}B_{CN}(E)\right] \tag{6}$$

where $\Gamma_\gamma(E)$ is the width of the γ-decay of an doorway 1^- state to the ground or the 2_1^+ state and Γ is the GDR width. The second term in eq. (6) corresponds to the compound decay.

Using the calculated structure of the 1^- states in the GDR region we can obtain microscopically both the cross section of excitation $\sigma_{\alpha,\alpha'}(E_{1^-_\nu})$ of each ν^{th} 1^- state and its decay width into the ground state or the 2_1^+ state. The GDR excitation at the KVI energies is dominated by the Coulomb term. Thus, we can approximate the form factor of excitation of the i^{th} one-phonon 1^- configuration by electromagnetic matrix elements $< 1_i^- \parallel E1 \parallel 0_{gs}^+ >$ multiplied by the energy-dependent part of the excitation cross section.

The decay width $\Gamma_\gamma(E_{1^-_\nu})$ of the ν^{th} 1^- excited state in eq. (6) is simply related to the γ-transition matrix elements between one-phonon configurations and the phonon vacuum for the decay into the ground state and between two-phonon and one-phonon configurations for the decay into the 2_1^+ state.

The exponential dependence of the Coulomb excitation cross section $\sigma_{\alpha,\alpha'}(E)$ as a function of excitation energy enhances strongly the lowest energies. As a result, the maximum in the $\sigma_{\alpha,\alpha'\gamma_0}(E)$ cross sections is shifted down compared to the E1 strength distribution. The calculated shape of both $\sigma_{\alpha,\alpha'\gamma_0}(E)$ and $\sigma_{\alpha,\alpha'\gamma_{2_1^+}}(E)$ cross sections is described rather well without introducing any averaging parameter. But the calculations underestimate the experimentally observed population of the 2_1^+ state in comparison with the ground state population by a factor 1.5-2.0. We have also estimated the contribution of excitation and decay of the GQR and the GMR to the total $(\alpha, \alpha'\gamma)$ cross section and found it to be equal to only a few percent.

4. EXCITATION OF DOUBLE GDR RESONANCES

The excitation of ^{136}Xe on ^{208}Pb target at E_{lab} = 690 MeV/n has recently been measured [15]. A prominent structure centered around twice the energy of the GDR was observed and interpreted as a multi-step excitation of the double GDR. Making use of the results of nuclear structure calculations within the QPM and of the theory of relativistic Coulomb excitation [16], the cross sections associated with the one-phonon giant resonances as well as two-step excitation of double resonances have been calculated [17]. These cross sections can be written in terms of the first- and second-order amplitudes $a^{(1)}$ and $a^{(2)}$ respectively as

$$\sigma^{(k)} = 2\pi \int_{R_{min}}^{\infty} bdb \int_0^{\infty} d\omega |\sum_{M_f} a^{(k)}_{I_f,M_f;I_o,M_o}(\omega,b)|^2 \ , k = 1,2, \tag{7}$$

For $k = 1$, the final states have angular momentum $I_f = 1$ for the GDR and $I_f = 2$ for the GQR, while for $k = 2$, both I_f =0 and 2 are possible. The amplitudes depend on the impact parameter b and on the excitation energy $\hbar\omega$. The first-order amplitude is equal to [16]

$$a^{(1)}_{I_f,M_f;I_o,M_o}(\omega) = \frac{4\pi Z_t e}{i\hbar(2\lambda+1)}(-1)^{I_o-M_o} \begin{pmatrix} I_o & \lambda & I_f \\ -M_o & M_o - M_f & M_f \end{pmatrix} < I_o||M(E\lambda)||I_f >$$

$$\times \ S_{\lambda,M_o-M_f}(\omega) \ , \tag{8}$$

where Z_t is the charge of the target. The radial integral S, carried out on a straight-line trajectory in keeping with the relativistic character of the reaction, is given by

$$S_{\lambda,\mu} = \frac{1}{4\pi v\gamma}(2\lambda+1)^{3/2} G_{E\lambda,\mu} \left(\frac{c}{v}\right) K_\mu(\xi(b)) \left(\frac{\omega}{c}\right)^{\lambda} \ . \tag{9}$$

Here $\xi(b) = \omega b/v\gamma$ is the adiabaticity parameter. The functions K_μ are modified Bessel functions, while the polynomials $G_{E\lambda,\mu}$ are related to the Legendre polynomials. The lower limit of integration over impact parameter is to be taken in such a way as to exclude nuclear reactions.

For the GDR we have used the B(E1) strength distribution calculated as described above in Sect. 3.1. The isoscalar and the isovector GQR have also been calculated within the same approach. The centroid, width and percentage of the EWSR associated with the isoscalar mode are 12.5 MeV, 3.2 MeV and 75% respectively. The corresponding quantities associated with the isovector GQR are 23.1 MeV, 3.6 MeV and 80%.

The second order amplitude needed in the calculation of the double phonon excitation can be written as

$$a^{(2)}_{I_f,M_f;I_o,M_o}(\omega_{fo}) = \frac{1}{2} \sum_{I_i,M_i} a^{(1)}_{I_f,M_f;I_i,M_i}(\omega_{fi}) a^{(1)}_{I_i,M_i;I_o,M_o}(\omega_{io})$$

$$+ \frac{i}{2\pi} \sum_{I_i,M_i} \mathcal{P} \int_{-\infty}^{\infty} \frac{dq}{q} a^{(1)}_{I_f,M_f;I_i,M_i}(\omega_{fi}-q) a^{(1)}_{I_i,M_i;I_o,M_o}(\omega_{io}+q) \ , \tag{10}$$

where $I_i M_i$ denotes the angular momentum and projection of the intermediate state. A central aspect of the above expression is the interference between the different E1-amplitudes, and thus between the different components of the dipole response (cf. eq.(2)). The principal integral in eq.(10) has been neglected in the calculations reported here. It vanishes for the excitation of a sharp dipole state, and is expected to give a small contribution even when the state has a finite width.

The evaluation of $a^{(2)}$ requires the knowledge of the matrix element $< I_f||M(E1)||I_i >$ $= < \nu_1\nu_2||M(E1)||\nu_1 >$. Because of the phonon character of the operators $Q_{\lambda\mu}$, it can be shown that

Table 1. Calculated for two values of r_o and experimental cross section (in mb) for the excitation of giant resonances in ^{136}Xe.

	GDR	$GQR_{\tau=0}$	$GQR_{\tau=1}$	GDR + GQR	$[GDR \otimes GDR]_{0^+,2^+}$
$r_o = 1.5$ fm	1480	110	60	1650	50
Experiment	–	–	–	1480	215 ± 50

$$< \nu_1\nu_2||M(E1)||\nu_1 >= \sqrt{1+\delta_{\nu_1\nu_2}} \sum_i R_i(\nu_2) < 0||Q_{1i}M(E1)||0 >$$

$$= \sqrt{1+\delta_{\nu_1\nu_2}} < \nu_2||M(E1)||0 > \ . \qquad (11)$$

This result emerges from the interference of 10^3 states, and shows that the strength function for the excitation of the double giant dipole resonance can be derived from the one-phonon strength function, considering the multiple excitation of all the $|\nu >$ states, with the appropriate boson factor and phase which account for the double excitation of the same state.

The resulting differential Coulomb-excitation cross sections associated with the two-phonon dipole excitation displays a centroid at 30.6 MeV, about twice that of the one-phonon 1^--states, while the width is $\Gamma \approx 6$ MeV, the ratio to that of the one-phonon excitation being 1.5.

The associated integrated values are displayed in Table 1, in comparison with the experimental findings. The value of the integrated cross section reported in ref. [15] is 1.85 ± 0.1 b. The nuclear contribution has been estimated to be about 100 mb, while about 3% (50 mb) of the cross section is found at higher energy. Subtracting these two contributions and the 2-phonon cross section leads to the value 1480 mb shown in the last row of Table 1.

As can be seen from Eq. (7), the calculated cross sections depend on the choice of the value of $R_{min} = r_o(A_p^{1/3} + A_t^{1/3})$. In keeping with the standard "safe distance", that is, the distance beyond which nuclear excitation can be safely neglected, we have used r_o = 1.5 fm. It is satisfactory that the measured cross section is rather close to this value. Also shown in Table 1 are the predictions associated with the sequential excitation of the double giant dipole resonance. The calculated value of 50 mb is a factor of 4 smaller than experimentally observed. Reducing r_o to 1.2 fm increases the cross section to 130 mb, a value which is still 50% smaller than the reported experimental value. The fact that the one-phonon cross section becomes a factor 1.7 larger than reported indicates that this way to proceed is likely not to be correct, and seems to be in contradiction with basic predictions of the harmonic picture of the GDR which is at the basis of the RPA description of these modes.

5. CONCLUSIONS

The Quasiparticle Phonon Model has been applied to calculations of the fine structure of giant resonances. The model Hamiltonian has been diagonalized on the basis of the wave functions of excited states which include one- and two-phonon configurations. The wave functions produced for each state contributing to a giant resonance allow one to consider different properties of single and double resonances on a microscopic basis.

REFERENCES

1. A. Van der Woude, Electric and Magnetic Giant Resonances in Nuclei, ed. J. Speth, World Scientific Publishing Company (1991) 99.
2. See many contributions on these subjects in the Proceedings of this Conference.
3. G.F. Bertsch, P.F. Bortignon and R.A. Broglia, Rev. Mod. Phys. **55** (1983) 287; J. Wambach, Rep. Prog. Phys. **51** (1988) 989.
4. A.I. Vdovin and V.G. Soloviev, Particles and Nuclei **14** (1983) 237.
5. V.V. Voronov and V.G. Soloviev, Particles and Nuclei **14** (1983) 1380.
6. V.G. Soloviev, Prog. in Part. and Nucl. Phys. **17** (1987) 107.
7. V.Yu. Ponomarev et al., Nucl. Phys. **A323** (1979) 446.
8. S.N. Belyaev et al., Sov. Journ. of Nucl. Phys. **55** (1992) 157.
9. V.G. Soloviev et al., Nucl. Phys. **A304** (1978) 503.
10. R.M. Laszewski et al., Phys. Rev. Lett. **61** (1988) 1710.
11. A. Krasznahorkay et al., Phys. Rev. Lett. **66** (1991) 1287.
12. V.Yu. Ponomarev and A. Krasznahorkay, Nucl. Phys. **A550** (1992) 150.
13. H. Feshbach, A. Kerman and S. Koonin, Ann. Phys. (N.Y.) **125** (1980) 429.
14. J.R. Beene et al., Phys. Rev. **C41** (1990) 920.
15. R. Schmidt et al., Phys. Rev. Lett. **70** (1993) 1767.
16. K. Alder and A. Winther, Nucl. Phys. **A319**(1979) 518.
17. V. Yu. Ponomarev et al., Preprint of the Niels Bohr Inst. (1993) NBI-93-40.